Geophys. J. R. astr. Soc. (1986) **86**, 563–588

Geomagnetic evidence for fluid upwelling at the core–mantle boundary

K. A. Whaler *Department of Earth Sciences, The University, Leeds LS2 9JT*

Accepted 1986 February 6. Received 1986 February 6; in original form 1985 June 24

Summary. Previous studies, both geomagnetic and seismic, have been unable to show conclusively whether or not there is fluid upwelling at the core–mantle boundary. Here a new method is developed, in which an attempt is made to invert geomagnetic secular variation data measured at the Earth's surface for a frozen-flux purely toroidal core–mantle boundary (CMB) velocity field, under the assumption that the mantle is electrically insulating and flux is frozen in at the CMB. These data have previously been inverted for the core–mantle boundary radial secular variation, from which the appropriate fit between model and data is known. Two different main field models were used to assess the effect of uncertainty in its radial component at the CMB. The conclusions were the same in both cases: frozen-flux purely toroidal motions provide a poor fit. A statistical test allows very firm rejection of the hypothesis that the residuals are not significantly larger, whereas there is no statistical difference between the residuals of inversions for radial secular variation and frozen-flux velocity fields at the CMB if upwelling and downwelling is included. The inherent non-uniqueness in the velocity field obtained is not of concern, since only their statistical properties are utilized and no physical significance is attached to the flows obtained.

Key words: core motions, secular variation, upwelling

1 Introduction

Although motion of the electrically conducting fluid of the outer core is now widely thought to be responsible for the Earth's magnetic field and its secular variation, attempts to invert magnetic data obtained at, or near, the Earth's surface for the details of the flow are fraught with difficulties. These problems are easier discussed in the context of the specific assumptions usually made in geomagnetism, which will now be introduced. The Earth's surface and core–mantle boundary (CMB) will both be assumed spherical and concentric; thus spherical polar coordinates (r, ϑ, ϕ) with origin at the Earth's centre are the natural coordinates to work in. The electrical conductivity of the core is sufficiently high that, on the time-scale of decades of interest in geomagnetism, it can be regarded as a perfect

conductor (Roberts & Scott 1965; Backus 1968). Thus the Ohmic diffusion term in the induction equation vanishes, giving

$$\dot{\mathbf{B}} = \nabla \times (\mathbf{v} \times \mathbf{B}) \tag{1}$$

where $\mathbf{B}$ is the magnetic field, $\dot{\mathbf{B}}$ its rate of change, $\mathbf{v}$ the velocity field.

In contrast, the electrical conductivity of the mantle is generally thought to be sufficiently low that it can be assumed perfectly insulating. Thus the magnetic field can be expressed as the gradient of a scalar potential throughout the mantle, there is an infinite jump in conductivity across the CMB, and hence only the radial component of the magnetic field is continuous across the interface, i.e. its value at the base of the mantle is the same as that at the top of the core. Deeper into the core, the presence of electric currents means the field cannot be extrapolated. Thus we are restricted to just the radial component of equation (1) only at the CMB itself which, with the boundary condition that $v_r = 0$ (no flow across the boundary), becomes

$$\dot{B}_r + \nabla_H \cdot (\mathbf{v} B_r) = 0$$

or

$$\dot{B}_r + \mathbf{v} \cdot \nabla_H B_r + B_r \nabla_H \cdot \mathbf{v} = 0 \tag{2}$$

where $\nabla_H = \nabla - \hat{\mathbf{r}}(\hat{\mathbf{r}} \cdot \nabla)$ contains only horizontal derivatives ($\hat{}$ denoting a unit vector). Backus showed that a necessary condition for the frozen-flux assumption to hold (which can be proved from equation (2)) is that

$$\int\int_{S_i} \dot{B}_r \, dS = 0 \tag{3}$$

where S_i is a patch of the CMB bounded by a null-flux curve (contour on which $B_r = 0$) and dS is an infinitesimal element of surface area, or equivalently, that the patch integrals of the radial main field component are time-invariant. The consequences of this will be considered later. Equation (2) indicates the nature of the task: from surface magnetic data, find B_r and $\dot{B}_r$ at the CMB and hence solve for $\mathbf{v}$. By further assuming that the core fluid is incompressible ($\nabla \cdot \mathbf{v} = 0$), the horizontal divergence of velocity, $\nabla_H \cdot \mathbf{v}$, can be interpreted as a measure of the amount of upwelling or downwelling of fluid at the CMB (Whaler 1980; Benton 1981), perhaps indicating the strength of convection there.

The problems of deducing the CMB fluid velocity, $\mathbf{v}$, from equation (2) fall into two classes. First, there is an inherent non-uniqueness in the velocity defined by (2), even with complete and perfect knowledge of B_r and $\dot{B}_r$ (Roberts & Scott 1965; Backus 1968). There is a whole class of velocity fields which do not generate any radial secular variation outside the core when interacting with the radial main field as described by equation (2). Several different testable assumptions about the nature of the CMB fluid flow have been developed which, if satisfied, reduce the non-uniqueness. These include the assumption of purely toroidal flow (i.e. motion without upwelling and downwelling) (Whaler 1980, 1982, 1984), steady toroidal flow (Gubbins 1982) and, more recently, the uniqueness of general steady flows has also been proved (Voorhies 1984). This paper is concerned with examining the possibility of purely toroidal motion from different angles to those discussed by Whaler (1980, 1982, 1984), which did not lead to any firm conclusions. A thermal history regime for the core in which there would be purely toroidal motion was discussed by Gubbins, Thomson & Whaler (1982).

The second problem to be faced when solving an equation such as (2) above is one common to all geophysical inverse problems – a finite quantity of inaccurate data cannot

uniquely determine an unknown function or set of parameters (Backus & Gilbert 1968). Thus, even if $\mathbf{v}$ in (2) was taken to represent just that part of the velocity function uniquely determined by the induction equation, it could not be unambiguously deduced due to the magnetic data limitations.

Efforts to determine the CMB velocity field geomagnetically continue despite these limitations, since no other data are as sensitive to the precise details of the flow.

Backus (1968) showed that, without further information or assumptions, the only uniquely determined part of the velocity field is that component perpendicular to null-flux curves. However, Whaler (1980) and Benton (1981) showed that, although the velocity itself is non-unique, some information on the rate of upwelling and downwelling of fluid can be obtained. From equation (2), where $\nabla_H B_r = 0$ (i.e. at local maxima, minima and saddle points of the radial field – collectively referred to as critical points in what follows),

$$\nabla_H \cdot \mathbf{v} = -\frac{\dot{B}_r}{B_r}.$$

Whaler (1980) further noticed, by superimposing contours on which $\dot{B}_r = 0$ on radial main field component maps of the CMB, that there appeared to be a tendency for contours on which $\dot{B}_r = 0$ to pass close to critical points, as if $\dot{B}_r = 0$ where $\nabla_H B_r = 0$. This suggests $\nabla_H \cdot \mathbf{v} = 0$, i.e. $\mathbf{v}$ is purely toroidal and there is no upwelling or downwelling of core fluid at the CMB. A statistical analysis backed this up (Whaler 1980, 1982). It is dangerous, however, to make assumptions concerning the form of the velocity field over the whole CMB on the basis of a few isolated point values (those at the critical points), especially as point measurements cannot be resolved (the best that can be done is a local average over the CMB centred on the point of interest). In this case, though, there are certain meaningful local averages that can be estimated without such severe lack of resolution: if $\nabla_H \cdot \mathbf{v} = 0$ then

$$\int\int_{S_j} \dot{B}_r \, dS = 0 \tag{4}$$

where S_j is a patch of the CMB bounded by any contour of B_r (except the null-flux curves whose integrals must vanish as a condition of the flux being frozen in). Whaler (1980) calculated integrals of this type from the 1965 IGRF (Zmuda 1971), but was unable to estimate their error bounds since there were no published errors on the spherical harmonic coefficients. Again, a statistical analysis gave no reason to reject the hypothesis that $\nabla_H \cdot \mathbf{v} = 0$.

Further calculations, using observatory data to calculate integrals of the form (4) directly, so that a resolution and error analysis could be performed, led to ambiguous results (Whaler 1984, hereafter referred to as paper 1). The error bounds on the integrals from the rather small number of data treated were sufficiently large that none of the integrals was significantly non-zero, but the range of possible values was so large that this could not really be regarded as a stringent test of the purely toroidal velocity hypothesis.

The calculations reported on here are another test of this hypothesis using an independent method on the same data as paper 1. Here it is assumed that the velocity field in (2) is purely toroidal, and then attempts are made to invert for it directly. A satisfactory inversion – where 'satisfactory' will be defined later – means there is no reason to reject the hypothesis. The non-uniqueness of the velocity field will not be of concern here since no attempt is made to attach physical significance to the motions obtained; instead, the uniquely determined CMB radial secular variation these flows generate is contoured as an aid to interpretation. Solving for a particular non-unique flow is undertaken purely to assess the

feasibility of the toroidal motions hypothesis. The indeterminate part of the toroidal velocity from equation (2) will clearly not affect the data inversion process and the assessment of the goodness-of-fit.

Some previous velocity inversion techniques are described briefly in the following section to facilitate comparison with the method to be used here, and some significant differences emerge. The inversion methods, which give solutions consistent with the necessary conditions (3) imposed by the frozen-flux hypothesis, are presented in Section 3, and the results are presented and discussed in terms of the original aims in Section 4.

2 The toroidal–poloidal velocity decomposition

Almost all previous studies of the CMB velocity field have made use of the toroidal–poloidal decomposition of the velocity field formulated by Roberts & Scott (1965). Since the velocity averages to zero over the CMB, it can be expressed in terms of two scalar functions of position on the sphere, S and T, which can be expanded in spherical harmonics:

$$\mathbf{v} = \mathbf{v}_T + \mathbf{v}_P$$

where

$$\mathbf{v}_T = \nabla \times (\mathbf{r}T) = \left(0, \frac{1}{\sin\vartheta}\frac{\partial T}{\partial \phi}, -\frac{\partial T}{\partial \vartheta}\right)$$

$$\mathbf{v}_P = \nabla (rS) = \left(0, \frac{\partial S}{\partial \vartheta}, \frac{1}{\sin\vartheta}\frac{\partial S}{\partial \phi}\right) \tag{5a}$$

and

$$T(\vartheta, \phi) = \sum_{l,m} t_l^m \, Y_l^m(\vartheta, \phi)$$

$$S(\vartheta, \phi) = \sum_{l,m} s_l^m \, Y_l^m(\vartheta, \phi) \tag{5b}$$

where $Y_l^m(\vartheta, \phi)$ is a spherical harmonic, temporarily assumed complex and fully normalized to simplify the notation. A notable exception to this formulation is that of Backus (1968) who decomposed $\mathbf{v}B_r$ (rather than just $\mathbf{v}$) into its toroidal and poloidal parts. The main advantage of expansion (5) over the Backus expression for the problem at hand is that the assumption of purely toroidal velocity can be made extremely simply.

Proceeding with the mathematical analysis for the moment, substitute (5) into (2) and, assuming both the main field and secular variation can be expanded in spherical harmonics, the following equation is obtained.

$$\sum_{l_1, m_1} \left(\frac{a}{c}\right)^{l_1+2} (l_1+1)\, \dot{g}_{l_1}^{m_1} Y_{l_1}^{m_1} = \frac{1}{c} \sum_{l_2, m_2} \sum_{l_3, m_3} \left(\frac{a}{c}\right)^{l_2+2} (l_2+1) g_{l_2}^{m_2}$$

$$\times \left[t_{l_3}^{m_3} / \sin\vartheta \left[\frac{\partial Y_{l_2}^{m_2}}{\partial \phi}\frac{\partial Y_{l_3}^{m_3}}{\partial \vartheta} - \frac{\partial Y_{l_2}^{m_2}}{\partial \vartheta}\frac{\partial Y_{l_3}^{m_3}}{\partial \phi} \right] \right.$$

$$\left. - s_{l_3}^{m_3} \left[\frac{\partial Y_{l_2}^{m_2}}{\partial \vartheta}\frac{\partial Y_{l_3}^{m_3}}{\partial \vartheta} + \frac{1}{\sin^2\vartheta}\frac{\partial Y_{l_2}^{m_2}}{\partial \phi}\frac{\partial Y_{l_3}^{m_3}}{\partial \phi} - l_3(l_3+1) Y_{l_2}^{m_2} Y_{l_3}^{m_3} \right] \right]$$

where a is the radius of the Earth (6371 km), c is the radius of the core (3485 km), and $\{\dot{g}_l^m\}$, $\{g_l^m\}$ are the spherical harmonic coefficients of the secular variation and main field respectively.

Multiplying by Y_l^{m*}, say (where * denotes the complex conjugate), integrating over the surface of the sphere and using the orthogonality of the spherical harmonics gives matrix equations relating the sets of spherical harmonic coefficients:

$$\dot{\mathbf{g}} = \mathbf{E}\mathbf{t} + \mathbf{G}\mathbf{s} = (\mathbf{E} : \mathbf{G}) \begin{pmatrix} \mathbf{t} \\ \cdots \\ \mathbf{s} \end{pmatrix} \tag{6}$$

where, after some algebra, the matrices $\mathbf{E}, \mathbf{G}$ have elements like

$$E_{l_1 l_3}^{m_1 m_3} = \frac{1}{c}\left(\frac{c}{a}\right)^{l_1+2} \frac{1}{l_1+1} \sum_{l_2, m_2} \left(\frac{a}{c}\right)^{l_2+2} (l_2+1) g_{l_2}^{m_2} \oint \left(\frac{\partial Y_{l_3}^{m_3}}{\partial \vartheta} \frac{\partial Y_{l_2}^{m_2}}{\partial \phi} - \frac{\partial Y_{l_2}^{m_2}}{\partial \vartheta} \frac{\partial Y_{l_3}^{m_3}}{\partial \phi} \right) Y_{l_1}^{m_1} d\Omega$$

$$G_{l_1 l_3}^{m_1 m_3} = \frac{2}{c}\left(\frac{c}{a}\right)^{l_1+2} \frac{1}{l_1+1} \sum_{l_2, m_2} \left(\frac{a}{c}\right)^{l_2+2} (l_2+1)\left[l_1(l_1+1) + l_3(l_3+1) - l_2(l_2+1)\right] g_{l_2}^{m_2}$$

$$\times \oint Y_{l_1}^{m_1} Y_{l_2}^{m_2} Y_{l_3}^{m_3} \, d\Omega$$

($\oint d\Omega$ denotes integration over the sphere) and $\dot{\mathbf{g}}$, $\mathbf{s}$ and $\mathbf{t}$ are vectors of spherical harmonic coefficients for the secular variation, S and T respectively, all suitably ordered. The integrals in the expressions for $\mathbf{E}$ and $\mathbf{G}$ are Elsasser and Gaunt integrals respectively (e.g. Gibson & Roberts 1969). They are expressible in closed form, and are non-zero only for certain pairs of (l_1, m_1), (l_2, m_2) and (l_3, m_3) values given by selection rules detailed by, e.g. Bullard & Gellman (1954). The most important of these in this problem is the triangle inequality, which states that l_1, l_2 and l_3 must form the sides of a triangle, i.e.

$$l_1 \leqslant l_2 + l_3$$

$$l_2 \leqslant l_1 + l_3$$

$$l_3 \leqslant l_1 + l_2$$

with the additional proviso that the sum of the l values must be even for Gaunt, and odd for Elsasser, integrals. This shows that, with the truncation level of the spherical harmonic expansion of any two of the main field, secular variation and velocity field fixed, the third is also determined.

Equations (6) form the basis of the inverse problem for CMB velocity calculations. With the spherical harmonic coefficients for the main field specified, one can solve for the vectors $\mathbf{t}$ and $\mathbf{s}$, or just $\mathbf{t}$ with $\mathbf{s} = 0$ if purely toroidal CMB velocity fields are sought, from secular variation data. The 'data' can be either spherical harmonic coefficients $\dot{\mathbf{g}}$ for the secular variation or, as discussed in Section 3, estimates of components of the scalar variation at isolated points at, or near, the Earth's surface (or a combination of the two).

Various velocity inversions using equations (6) have been reported in the literature. Kahle, Vestine & Ball (1967) (and subsequent papers by the same authors) performed a straightforward least squares inversion of main field and secular variation coefficients for the spherical harmonic coefficients of S and T up to degree and order 4. They found instabilities developed when extrapolating the geomagnetic field to the CMB, and their results are also subject to severe truncation effects now well known in spherical harmonic analysis.

More recently, Madden & Le Mouël (1982) performed a damped least squares inversion to reduce the problems of truncation of the spherical harmonic expansions of S and T, using a combination of measurements and spherical harmonic models of the secular variation. They also examined how well these data resolved the spherical harmonic coefficients obtained, and found that the poloidal coefficients, $\{s_l^m\}$, were better resolved than the toroidal ones, $\{t_l^m\}$. This, they argued, was due to the precise form of the non-uniqueness of the velocity field. Any poloidal velocity vectors in the null space, i.e. poloidal velocities which do not generate any secular variation outside the core, are pathological, and therefore there is unlikely to be a contribution from them in the damped least squares solution, which is regular everywhere. However, the toroidal null-space velocities are regular and thus may contribute to the solution obtained. Madden & Le Mouël (1982) state that, since the damped inverse solution is minimum norm, i.e. it minimizes a measure of the 'length' of the velocity vector, the null-space contribution might be reduced, although the reasoning is not clear. Thus their argument is that the velocity field they calculate, which extends to harmonic degree 5, is a good estimate of that part of the actual CMB motion which is uniquely determined by the data.

Higher harmonic degree motions (up to degree and order 9) have been obtained by Gire, Le Mouël & Madden (1984, 1986), using the method of Madden & Le Mouël (1982) with some extensions and refinements. Gire *et al.* (1984) were investigating the westward drift rate of the geomagnetic field, and were thus primarily interested in the toroidal coefficient t_1^0. Due to the stabilizing effects of the methods of analysis they used, t_1^0 had similar values, and was reasonably well-resolved, regardless of the details of the inversion. These conclusions apply to many of the other low degree and order coefficients in the expansion (Gire *et al.* 1986).

Voorhies (1984) used published spherical harmonic models of the main field and secular variation to estimate steady motions, whose uniqueness has been proved (Voorhies & Backus 1985). The method followed that of Kahle *et al.* (1967) closely, i.e. an inversion for the coefficients of a truncated spherical harmonic expansion that best fit, in both the spatial and temporal least squares sense, a model of the time-varying geomagnetic field. Voorhies obtained both purely toroidal and complete (i.e. toroidal and poloidal) flows, but concluded that an inadequate fit was obtained without including poloidal terms.

When investigating the purely toroidal velocity hypothesis, there are disadvantages to the methods outlined above. First, for non-orthogonal data (always the case in practice), truncation of the spherical harmonic series followed by straightforward least squares inversion leads to solutions that are strongly dependent on the particular truncation level chosen. Changing the truncation level changes all the coefficients, due to spatial aliasing of the higher-order harmonics. This is particularly severe when downward continuation is involved, because of the preferential amplification of the shorter wavelength components (Whaler & Gubbins 1981).

Secondly, problems arise when trying to test hypotheses using spherical harmonic models for the secular variation, rather than original data. It is impossible to tell whether failure to satisfy, say, the purely toroidal velocity assumption, is due to the failure of the assumption itself or the failure of the spherical harmonic model to fit the data it represents. For these reasons it is better to work with secular variation measurements and, if spherical harmonic coefficients are used, to attach a low weight to them.

Previous investigators do not generally appear to have used the triangle inequality for Gaunt and Elsasser integrals to determine the truncation level of the spherical harmonic series for the velocity. If spherical harmonic models are taken to represent both the main field and the secular variation, velocity coefficients can extend to harmonic degree given by

the sum of those of the main field and secular variation models (or that sum minus one for purely toroidal motion, since that part of the flow involves Elsasser integrals – see equations (6) – which vanish unless the sum of the harmonic degree value is odd). Most published velocity models have been truncated lower than this, usually considerably lower. This would be justifiable if the velocity model converged at the chosen truncation level, but in the few instances where this has been investigated (e.g. Voorhies 1984), this has not been found to be the case. The results of this paper suggest it is unlikely that any of the previously derived spherical harmonic series for the CMB velocity field have converged. Specifying the truncation level for the velocity field below its maximum value determined by the triangle inequality for the Gaunt and Elsasser integrals only serves to introduce a further, unnecessary, parameter into the solution and provide another source of ambiguity in the results.

If, on the other hand, 'raw' secular variation data are to be inverted for the CMB velocity field, there are no constraints on the maximum harmonic degree of the velocity coefficients. This maximum value, however, taken in conjunction with the truncation level of the main field, indicates to what harmonic degree the secular variation this velocity field generates by advection of field lines will run. The CMB secular variation field, which is unaffected by the non-uniqueness in the velocity, can then be compared with other models to gauge its acceptability; hence the acceptability of the constraints on the velocity field it was produced by can also be assessed.

Another disadvantage of using spherical harmonic models over original secular variation data is that the extent to which the model should fit the 'data', i.e. the secular variation coefficients, is difficult to ascertain. Some progress could be made using the covariance matrix from the original inversion of the raw data, but this is cumbersome and the covariance matrix is often unavailable.

For the reasons outlined above, the approach taken here differs from previous velocity determinations in several important respects. The data are estimates of secular variation components, with associated errors, rather than spherical harmonic models. The expected fit of the model to the data is known from previous inversions, e.g. those in paper 1, which also enables the CMB secular variation generated by the velocity field advecting field lines to be compared to direct CMB secular variation inversions. The truncation level of the secular variation field is determined from those of the chosen main field model and that specified in the velocity inversion by the triangle inequality. An aim of the analysis was to obtain convergent spherical harmonic series, for which the velocity model runs to relatively high harmonic degree, so that raising the harmonic degree does not change the values of the coefficients, or alter the goodness-of-fit of the solution, etc. Details of the ways in which solutions were obtained are given in the next section. Purely toroidal solutions were obtained by removing $\mathbf{G}$ and $\mathbf{s}$ from (6) and inverting only for $\mathbf{t}$. These models were compared with other solutions, both those of paper 1 and other velocity inversions including poloidal coefficients, to assess the 'no-upwelling' hypothesis.

3 Stochastic inversion for velocity coefficients

The method used to determine the velocity coefficients was stochastic inversion, first used in spherical harmonic analysis by Gubbins (1983), in which further details can be found. It is also similar to the methods of Madden & Le Mouël (1982) and Gire *et al.* (1984, 1986). The notation of Gubbins (1983) will be followed quite closely. Equations (6) relating secular

variation coefficients to velocity coefficients can be rewritten.

$$\dot{\mathbf{g}} = \mathbf{B}\mathbf{m}, \tag{7}$$

where

$$\mathbf{B} = \begin{cases} (\mathbf{E} : \mathbf{G}) \text{ for toroidal and poloidal flows} \\ \mathbf{E} \text{ for purely toroidal motion} \end{cases}$$

and

$$\mathbf{m} = \begin{cases} \begin{pmatrix} \mathbf{t} \\ \cdots \\ \mathbf{s} \end{pmatrix} \text{ for combined flows} \\ \mathbf{t} \text{ for purely toroidal motion.} \end{cases}$$

Winch (1974) has expressed the Gaunt and Elsasser integrals in closed form in terms of the Wigner 3-*j* coefficients of quantum mechanics (Wigner 1959), and has written a FORTRAN function to evaluate the 3-*j* coefficients. For the normalization of spherical harmonics he chose, the results can be relatively simply recast into Schmidt quasi-normalization recommended in geomagnetism (Winch 1974; Winch & Bamber, unpublished manuscript). Thus, the elements of the matrices **E** and **G** in (7) could be rapidly and accurately calculated using the supplied FORTRAN function, with published values of the spherical harmonic coefficients of the main field. The results were checked by comparison with approximate numerical integration, ensuring that the renormalization had been performed correctly.

Secular variation coefficients, $\dot{\mathbf{g}}$, can be related to surface secular variation data, γ (measurements of $\dot{B}_r$, $\dot{B}_\vartheta$ and $\dot{B}_\phi$ at permanent magnetic observatories in this case) by

$$\gamma = \mathbf{Y}\dot{\mathbf{g}}. \tag{8}$$

Where the elements of **Y** (of three types, corresponding to the three components measured) are multiples of spherical harmonics and their ϑ and ϕ derivatives. Combining (7) and (8), the data are related to the model by

$$\gamma = \mathbf{Y}\dot{\mathbf{g}} = \mathbf{Y}\mathbf{B}\mathbf{m} = \mathbf{A}\mathbf{m} \tag{9}$$

where $\mathbf{A} = \mathbf{Y}\mathbf{B}$.

Then (Gubbins 1983) the stochastic inverse solution for $\mathbf{m}$, $\hat{\mathbf{m}}$ say, is

$$\hat{\mathbf{m}} = (\mathbf{A}^T\mathbf{C}_e^{-1}\mathbf{A} + \mathbf{C}_m^{-1})^{-1}\mathbf{A}^T\mathbf{C}_e^{-1}\gamma \tag{10}$$

where $\mathbf{C}_e$ is the data covariance matrix and $\mathbf{C}_m$ is the *a priori* covariance matrix of the model.

All linear systems of type (10) were solved by Cholesky decomposition and back substitution. As usually is the case, the data are assumed uncorrelated, so the covariance matrix of the data is diagonal, with their variances the diagonal elements. The *a priori* model covariance matrix is chosen to reflect our prejudices about the expected model. In this case they include our wish that the model converges, which in turn governs the shape of the power spectrum at high harmonic degree, beyond the influence of the data. There is initially no *a priori* reason to expect the model parameters to be correlated, so C_m is diagonal, where each diagonal element depends on the harmonic degree (but not order) of the coefficient it is associated with. For example, following Gubbins (1983), we might require that each harmonic degree contributes equally to the variance of the quantity of interest – in Gubbins' (1983) case, the CMB radial secular variation field, here the CMB velocity field. Using the orthogonality of the spherical harmonics, where now we have reverted to Schmidt quasi-

normalized form,

$$(\delta v_T)^2 = 2\pi \sum_l l(l+1) \sum_{m=0}^{l} (\delta t_l^m)^2$$

$$(\delta v_P)^2 = 2\pi \sum_l l(l+1) \sum_{m=0}^{l} (\delta s_l^m)^2 \tag{11}$$

where δv_T^2 is the variance of the toroidal velocity field, $\delta t_l^{m^2}$ the variance of a toroidal velocity coefficient, and similarly for the poloidal velocity field. We do not expect any dependence on orientation, i.e. on harmonic order m, so if we further assume that all coefficients of the same harmonic degree have the same variance, σ_l^2, we see that, for each harmonic degree to contribute equally to the variance of the velocity field.

$$\sigma_l^2 \propto \frac{1}{l(l+1)}. \tag{12}$$

Thus we choose *a priori*

$$\mathbf{C}_m^{-1} = \lambda \mathbf{Q}$$

where

$$Q_{ij} = l(l+1)\delta_{ij} \tag{13}$$

δ_{ij} being the Kronecker delta, and the elements of $\mathbf{Q}$ are arranged according to spherical harmonic order and degree in the same way as the model parameters.

Another choice of *a priori* information could be obtained by requiring that the solution for $\mathbf{v}$ be spatially smooth, e.g. that it minimizes $\oint_{CMB} \mathbf{v}^2 d\Omega$, where $\oint_{CMB} d\Omega$ denotes integration over the CMB, for a given fit to the data. Again, using the orthogonality of the spherical harmonics, it can be shown that

$$\oint_{CMB} \mathbf{v}^2 d\Omega = 4\pi \sum_l \frac{l(l+1)}{2l+1} \sum_{m=0}^{l} [(t_l^m)^2 + (s_l^m)^2]. \tag{14}$$

This will tend to smooth, or stabilize, the inversion, since (14) discriminates against large (absolute) values of the velocity coefficients, especially at high harmonic degree. In this case, then, the *a priori* covariance matrix would be

$$\mathbf{C}_m^{-1} = \lambda \mathbf{Q}$$

where

$$Q_{ij} = \frac{l(l+1)}{2l+1}\delta_{ij} \tag{15}$$

ordered as before. This illustrates another interpretation of the stochastic inverse solution – it is also a minimum norm solution, minimizing the *solution norm*

$$\hat{\mathbf{m}}^T \mathbf{C}_m^{-1} \hat{\mathbf{m}} = \lambda \hat{\mathbf{m}}^T \mathbf{Q} \hat{\mathbf{m}}$$

for given *residual norm*

$$\mathbf{e}^T \mathbf{C}_e^{-1} \mathbf{e}$$

where $\mathbf{e} = \gamma - \hat{\gamma}$ is the residual vector, and $\hat{\gamma} = \mathbf{A}\hat{\mathbf{m}}$ are the predictions of the data by the

model, the relative emphasis on obtaining a good fit to the data (represented by a small value of the residual norm) or a smooth solution (a small value of the solution norm) being controlled by the arbitrary multiplier λ. The residual norm therefore quantifies the fit to the data, and should be distributed as χ^2_n, where n is the number of data. In inversion for spherical harmonic coefficients of the CMB magnetic field or its secular variation (e.g. Gubbins 1983, 1984; Gubbins & Bloxham 1985; Bloxham & Gubbins 1986), the geometrical attenuation/amplification factor $(a/c)^{l+2}$ dominates all reasonable choices of *a priori* information, making the solution almost totally insensitive to the norm chosen, and also ensuring convergence at fairly low harmonic degree. By contrast, the elements of $\mathbf{Q} \sim l^2$ and l for choices (13) and (15) of $\mathbf{C}_\mathbf{m}$ respectively, so different choices of *a priori* information for velocity inversions have a more marked effect on the solution obtained, as will be seen in the following section.

Previous inversions for the CMB radial secular variation field (e.g. paper 1), using the dataset also considered here, suggest a residual norm $(\mathbf{e}^\mathrm{T}\mathbf{C}_\mathbf{e}^{-1}\mathbf{e}$, or

$$\left\{\sum_{i=1}^{n}\frac{e_i}{\sigma_i}\right\}^2,$$

where σ_i is the standard error on γ_i, under the assumption of uncorrelated errors made here) of about 1300 is appropriate. This is a factor of about 4 greater than the expected value of 318 (the number of data), which, as discussed in Shure *et al.* (1983), may be due to external geomagnetic effects contaminating the data. Once a solution for the velocity coefficients, $\hat{\mathbf{m}}$, has been calculated, with the appropriate residual norm, it can be multiplied by the matrix $\mathbf{B}$ (see (7)) to obtain the secular variation coefficients, which should also be a convergent series if the velocity series is (and, in fact, is likely to converge faster than the velocity).

The inversions for the CMB secular variation field in paper 1 minimized a norm of the secular variation field

$$\oint_{\mathrm{CMB}} \dot{B}_\mathrm{r}^2\, d\Omega = 4\pi \sum_l \left(\frac{a}{c}\right)^{2l+4} \frac{(l+1)^2}{2l+1} \sum_{m=0}^{l} \dot{g}_l^{m\,2} \tag{16}$$

which can also be calculated from the predicted secular variation coefficients $\dot{\mathbf{g}}$ determined from $\hat{\mathbf{m}}$. As these are solutions which minimize velocity, rather than CMB secular variation, norms, this quantity will not in general be small. However, it is possible to minimize the norm $\oint_{\mathrm{CMB}} \dot{B}_\mathrm{r}^2\, d\Omega$ when calculating velocity solutions by an appropriate choice of *a priori* covariance matrix $\mathbf{C}_\mathrm{m}$. This is a norm minimizing a uniquely determined, physically meaningful quantity, unlike the two earlier choices. The objective function to be minimized in this case is

$$\mathbf{e}^\mathrm{T}\mathbf{C}_\mathbf{e}^{-1}\mathbf{e} + \mu \oint_{\mathrm{CMB}} \dot{B}_\mathrm{r}^2\, d\Omega$$

where μ acts as a trade-off parameter

$$= \mathbf{e}^\mathrm{T}\mathbf{C}_\mathbf{e}^{-1}\mathbf{e} + \dot{\mathbf{g}}^\mathrm{T}\dot{\mathbf{Q}}\dot{\mathbf{g}}$$

where $\dot{\mathbf{Q}}$ is diagonal with elements

$$4\pi\mu \left(\frac{a}{c}\right)^{2l+4} \frac{(l+1)^2}{2l+1}$$

(by 16)

$$= \mathbf{e}^\mathrm{T}\mathbf{C}_\mathbf{e}^{-1}\mathbf{e} + \mathbf{m}^\mathrm{T}\mathbf{B}^\mathrm{T}\dot{\mathbf{Q}}\mathbf{B}\mathbf{m}$$

(using 7), which leads to the solution

$$\hat{\mathbf{m}} = (\mathbf{A}^T \mathbf{C}_e^{-1} \mathbf{A} + \mathbf{B}^T \dot{\mathbf{Q}} \mathbf{B})^{-1} \mathbf{A}^T \mathbf{C}_e^{-1} \gamma. \tag{17}$$

Thus $\mathbf{C}_m^{-1} = \mathbf{B}^T \dot{\mathbf{Q}} \mathbf{B}$, which is positive definite symmetric, since $\dot{\mathbf{Q}}$ is diagonal, but not itself diagonal. Whereas in most cases stochastic inversion involves adding numbers to the diagonal of the undamped normal equations matrix, a common method of stabilizing least squares inversion, here *every* element of the normal equations matrix is modified. In practice, it was found that, although the modified matrix to be inverted, $\mathbf{A}^T \mathbf{C}_e^{-1} \mathbf{A} + \mathbf{B}^T \dot{\mathbf{Q}} \mathbf{B}$, is strictly algebraically positive definite, it was not numerically so. This problem was circumvented by including in the objective function one of the norms of the velocity field introduced earlier, with an extremely small (fixed) weight, i.e. the objective function was, instead,

$$\mathbf{e}^T \mathbf{C}_e^{-1} \mathbf{e} + \mu \oint_{CMB} \dot{B}_r^2 \, d\Omega + \lambda \mathbf{m}^T \mathbf{Q} \mathbf{m} \tag{18}$$

where $\mathbf{Q}$ has one of the forms (13) or (15), and λ was set at an extremely small value – as little as 10 orders of magnitude down (all calculations being in double precision) on its value when using (13) or (15) was sufficient to achieve a solution numerically. The effect of the extra term should be small, and the solution so obtained therefore very nearly minimum $\oint_{CMB} \dot{B}_r^2 \, d\Omega$ for fixed residual norm, a claim borne out in the following section. The secular variation field predicted by the velocity fields determined in this fashion can be compared directly with their counterparts obtained by inversion of the same data for secular variation coefficients with the same norm. Any other *a priori* information on $\dot{\mathbf{B}}$ (e.g. other alternatives considered by Gubbins 1983) could be incorporated by an appropriate choice of $\dot{\mathbf{Q}}$ in (17).

4 Results

The data were inverted under the assumptions made in the Introduction, i.e. that the electrical conductivity of the mantle vanishes, and that of the core is very large. Thus, the main field at the CMB is known exactly, as given by the downward continued, truncated spherical harmonic expansion. Corrections to both the main field and secular variation, on downward continuation to the CMB, are small for likely conductivity profiles (Benton & Whaler 1983), so the former assumption should not seriously affect the results. An attempt to assess the effect of the latter assumption was made by using two independent models of the main field, which had a markedly different CMB radial field configuration and hence a different set of null-flux curves. Therefore, they would not both be consistent with the frozen-flux hypothesis. The first was the DGRF for 1965 (Barraclough *et al.* 1978), which extends to harmonic degree 8, and was also the main field used in the calculations of paper 1. Its null-flux curve configuration is considerably simpler than that for models for 1980 based on large quantities of high quality *MAGSAT* data. On the assumption that the models for 1980 are the closest to true field, the 1965 DGRF is not consistent with the frozen-flux hypothesis, since the null-flux patch integrals are not conserved. Gubbins (1985, private communication) has produced an alternative model for the earlier epoch (actually, 1966 rather than 1965), which has the same set of null-flux curves as the *MAGSAT* models. This model extends to harmonic degree 20, but a map of the CMB radial field component obtained by taking terms up to degree and order 12 only was virtually indistinguishable from that produced by the complete set. Therefore, to reduce the computational effort, the smaller set of coefficients was used to define the second model, which will be denoted N1966(12) in what follows. The CMB radial component of the two models is contoured in Fig. 1. The null-flux patch integrals of the radial component for this model are given in

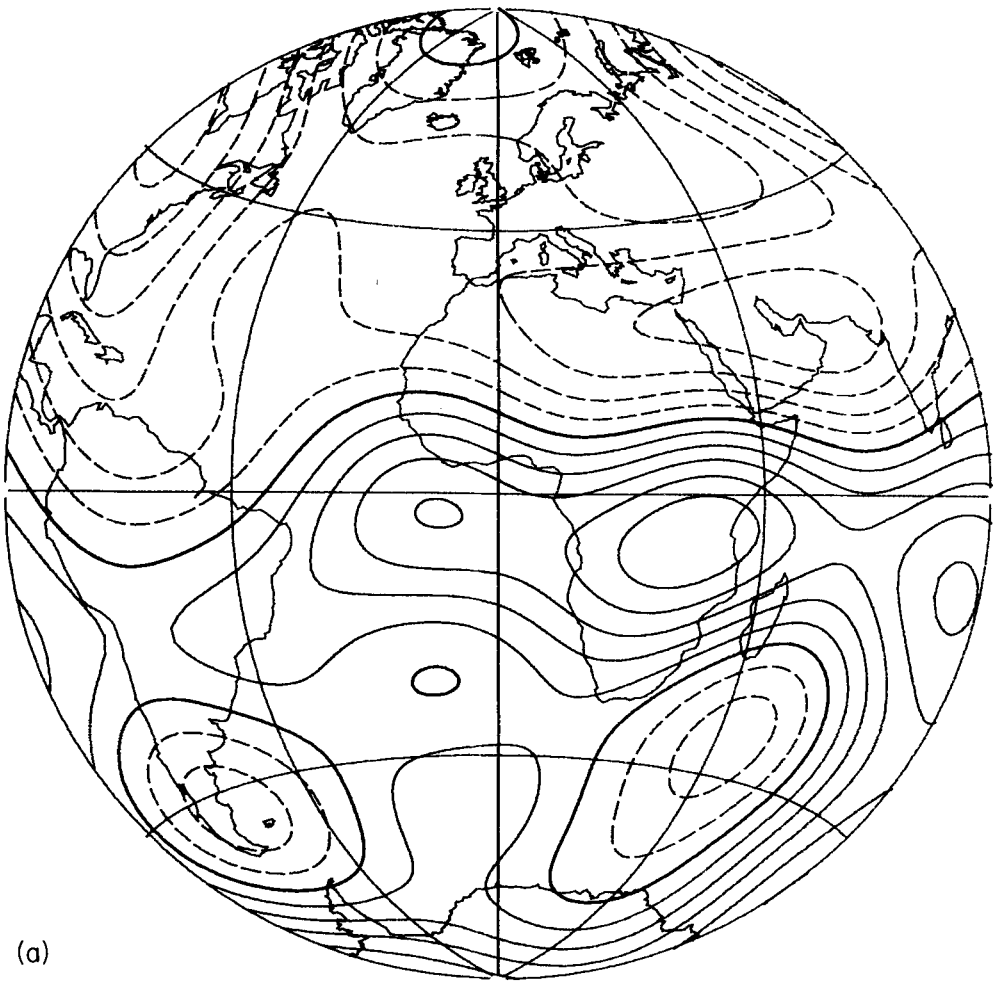

Figure 1. The CMB radial component of the main field models used here, contoured on a Lambert equal area projection. The contour interval is 100 μT. Positive contours continuous, negative contours dashed, thicker lines are zero contours. Coastlines at the Earth's surface are included for reference. (a) DGRF 1965, (b) N1966(12).

Table 1, together with those for Gubbins & Bloxham's (1985) model for 1980, based on *MAGSAT* data, taken from Bloxham & Gubbins (1986). The method by which the patch integrals for 1966 were calculated differs slightly from the previous methods, and is described more fully later in this section. The difference between the two methods is greatest for integrals over the almost hemispheric patches, numbers 1 and 2 in Table 1. The rather large changes in these two patch integrals between the two epochs are probably not significant. The value of patch integral number 3, over the region of the core beneath the South Atlantic, hardly alters between these two epochs, which provided the strongest evidence for flux diffusion in Bloxham & Gubbins' (1986) analysis. However, using the statistical test described by Bloxham & Gubbins (1986), it appears that this model, too, is inconsistent with the frozen-flux hypothesis. As there is no simple way in which errors on

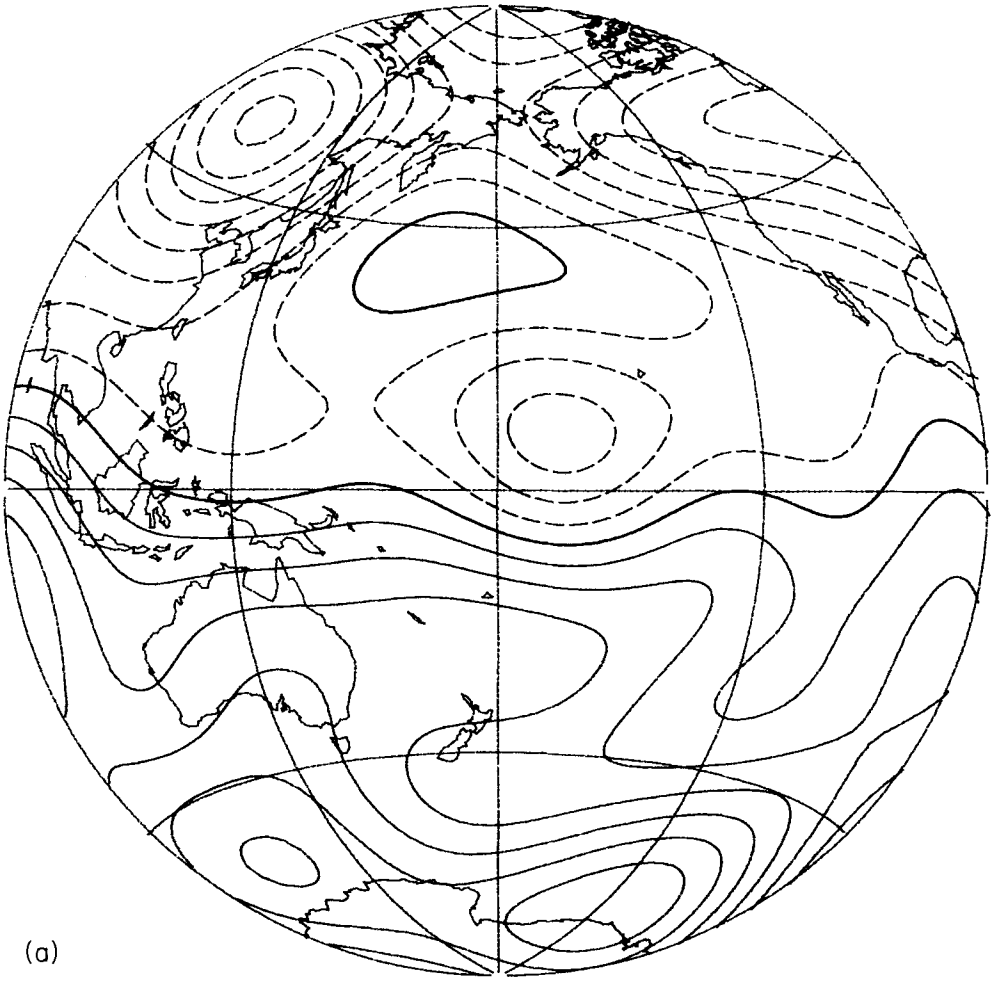

Figure 1 – *continued*

Table 1. Integrals of the radial main field component over patches bounded by null-flux curves for Gubbins & Bloxham's (1985) model for 1980 and N1966(12) (Gubbins, private communication). Values are in MWb.

	Patch	1980	1966	80–66	Error 86–66
1	Northern hemisphere	−17 547	−17 259	−288	38
2	Southern hemisphere	18 850	18 501	349	43
3	South Atlantic	−1 274	−1 239	−35	27
4	St Helena	−88	−57	−31	13
5	Easter Island	−20	−22	2	12
6	North Atlantic	3	7	−4	6
7	North-west Pacific	2	27	−25	13
8	North-east Pacific	33	5	28	7
9	North Pole	39	37	2	12

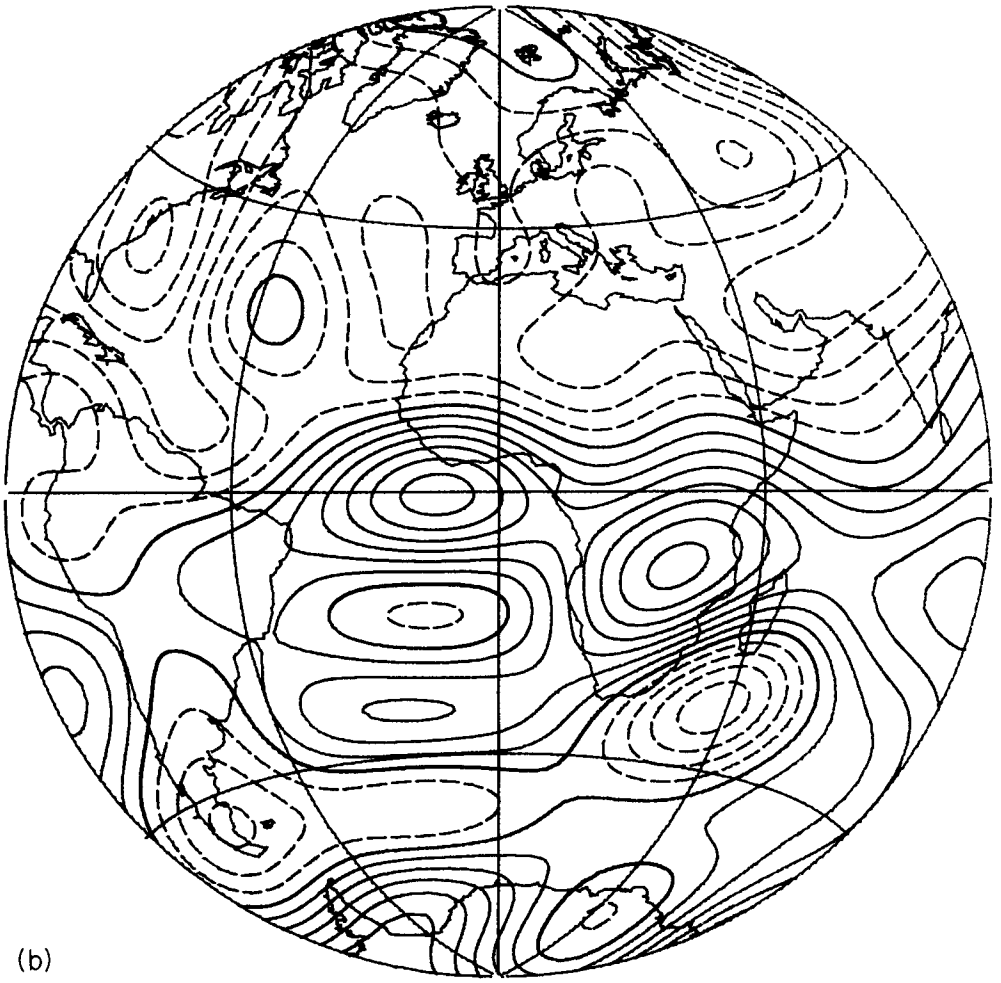

Figure 1 – *continued*

the downward continued main field, i.e. in the equations of condition relating the model to the data, can be taken into account in the inversion scheme proposed here, the differences between the results with these two models will be used to indicate how the uncertainty in **B** affects the conclusions.

Purely toroidal velocity solutions were sought initially, in keeping with the underlying aim of assessing whether they were acceptable models of the data. The required normalized sum of squares of residuals was 1302, for which the minimum $\oint_{CMB} \dot{B}_r^2 \, d\Omega$ value was $67.8 \times 10^6 \, nT^2 \, yr^{-2}$ (see paper 1) using the same data. Inversions at successive truncation levels for the toroidal velocity field coefficients showed that convergence (to at least three significant figures) was achieved at about harmonic degree 18 (for the sum of squares of residuals of paper 1) with the first two norms, (13) and (15) discussed in the previous section. As the main field models used run to harmonic degree 8 and 12, the fluid motions will therefore produce secular variation up to harmonic degree 25 and 29 respectively by advecting the field lines, which is considerably higher than the truncation level of 20 by which previously

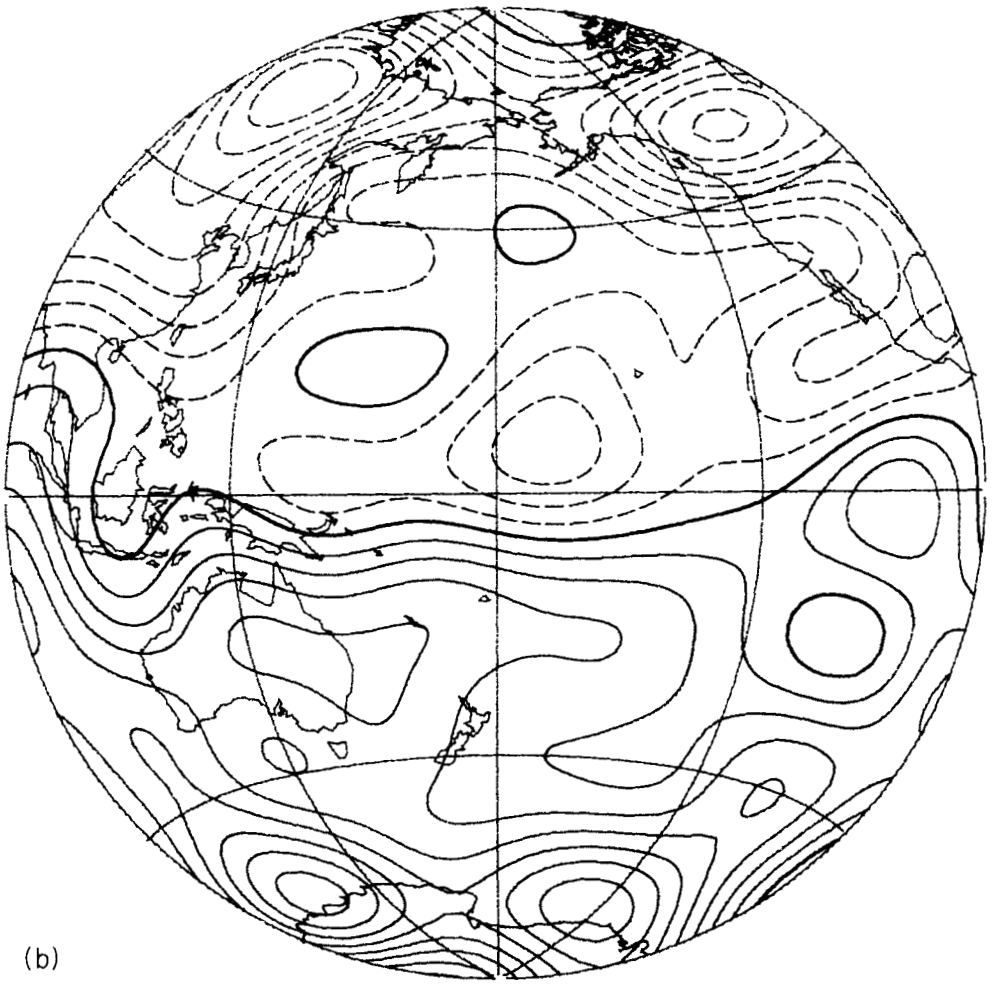

Figure 1 – *continued*

calculated secular variation models had converged (e.g. Gubbins 1983). The predicted secular variation coefficients from the models produced by norms (13) and (15) also form a convergent spherical harmonic series, with $\oint_{CMB} \dot{B}_r^2 \, d\Omega$ values of 257 and 275 respectively using the DGRF, and 277 for both norms using N1966(12). Here and in what follows, values of $\oint_{CMB} \dot{B}_r^2 \, d\Omega$ will be quoted in units of $10^6 \mathrm{nT}^2 \mathrm{yr}^{-2}$. Convergence of the secular variation series is easily seen in the power spectra for the four models, shown in Fig. 2, although they have not converged by harmonic degree 20. The velocity spectra, also shown, plot the contribution to $\oint_{CMB} \mathbf{v}^2 \, d\Omega$ from coefficients of degree l, i.e.

$$\frac{4\pi l(l+1)}{2l+1} \sum_{m=0}^{l} (t_l^m)^2$$

versus degree, l. Note that the velocity power spectra are plotted on linear axes; those for the CMB secular variation are log-linear. That the velocity models have converged is less obvious

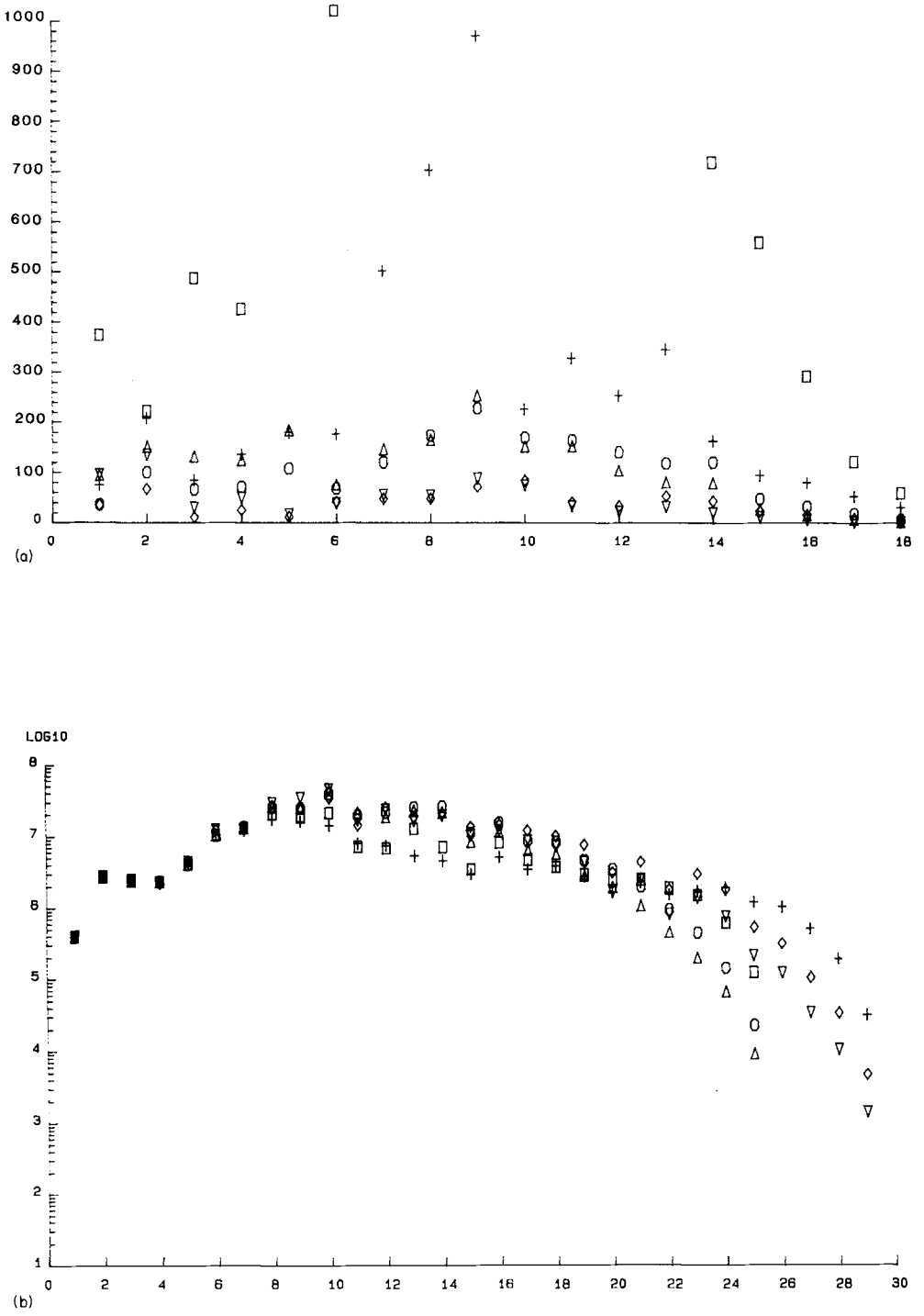

Figure 2. Power spectra of (a) the CMB velocity field and (b) radial CMB secular variation for purely toroidal models T1–6. All have a residual norm of 1302, T1, Δ; T2, ○; T3, □; T5, ▽; T6, ◆; T7, +. Points for T3 between harmonic degrees 7 and 13 inclusive are off the vertical scale in (a).

from these plots, but the linear trend of the last segment suggests the *a priori* information takes over at about harmonic degree 15. They also show that the flow is weaker when model N1966(12) is used to define the main field. The considerably larger values of $\oint_{CMB}\dot{B}_r^2\,d\Omega$ than that obtained in paper 1 for these four models are reflected in the roughness of the CMB secular variation; a typical example of the radial component is contoured in Fig. 3. However, the same broad features to those in the maps of paper 1 are apparent. Numbers characterizing the models (e.g. their solution norms) are summarized in Table 2.

Table 2. Summary of the numbers characterizing the models presented here, and those of the comparison model from paper 1.

Model	Solution for	Max. degree of main field	Max. degree of solution	solution norm minimised*	damping parameter, λ	Residual norm	$\oint_{CMB}\underline{v}^2 d\Omega$ (km^2yr^{-2})	$\oint_{CMB}\dot{B}_r^2 d\Omega$ ($10^6 nT^2yr^{-2}$)
Paper 1	CMB $\dot{B}_r$	-	-	$\oint_{CMB}\dot{B}_r^2 d\Omega$	-	1302	-	67.8
T1	$\underline{t}$	8	18	(13)	.179	1302	1951	257.4
T2	$\underline{t}$	8	18	(15)	.332	1302	1792	275.2
T3	$\underline{t}$	8	18	(18)	3.32×10^{-6}	1302	34.48×10^3	162.7
T4	$\underline{t}$	8	18	(18)	5.52×10^{-6}	2607	21.88×10^3	67.8
T5	$\underline{t}$	12	18	(13)	.630	1302	770.2	276.7
T6	$\underline{t}$	12	18	(15)	1.08	1302	668.6	276.7
T7	$\underline{t}$	12	18	(18)	4.30×10^{-6}	1302	4619	139.0
T8	$\underline{t}$	12	18	(18)	6.935×10^{-5}	2592	2479	67.8
TP1	$\underline{t},\underline{s}$	8	18	(13)	3.52	1302	340.6	111.7
TP2	$\underline{t},\underline{s}$	8	18	(15)	5.05	1302	272.4	145.8
TP3	$\underline{t},\underline{s}$	8	18	(18)	8.875×10^{-6}	1302	1164	71.0
TP4	$\underline{t},\underline{s}$	8	18	(18)	1.025×10^{-6}	1332	1127	67.8
TP5	$\underline{t},\underline{s}$	12	18	(13)	5.05	1302	268.3	136.2
TP6	$\underline{t},\underline{s}$	12	18	(15)	6.77	1302	202.1	176.0
TP7	$\underline{t},\underline{s}$	12	18	(18)	8.4×10^{-6}	1302	1892	81.6
TP8	$\underline{t},\underline{s}$	12	18	(18)	1.56×10^{-5}	1460	1738	67.8

* Numbers in brackets refer to equations numbered in the text.

There is no obvious way to compare the four solutions obtained here with that of paper 1 to assess the 'no upwelling' hypothesis, since comparing solutions e.g. minimizing $\oint_{CMB}\mathbf{v}^2\,d\Omega$ with those minimizing $\oint_{CMB}\dot{B}_r^2\,d\Omega$ is not comparing like with like. Minimizing the norms (13) and (15) of $\mathbf{v}$ does not lead to solutions with small $\oint_{CMB}\dot{B}_r^2\,d\Omega$ as well. This prompted development of the norm (18) minimizing (or nearly minimizing) $\oint_{CMB}\dot{B}_r^2\,d\Omega$ when inverting for velocity coefficients described in the previous section. We would not expect to obtain values of $\oint_{CMB}\dot{B}_r^2\,d\Omega$ quite as small as those of paper 1 since we had to stabilize the solutions numerically by adding extra weight to the diagonal elements, but this will not turn out to be crucial in what follows.

The minimum values of $\oint_{CMB}\dot{B}_r^2\,d\Omega$ for purely toroidal motion with a residual norm of 1302 were found to be 163 (with the DGRF main field model) and 139 (N1966(12)), about two-thirds or a half of those of the previous solutions, but still a factor 2 larger than with direct inversion for CMB radial secular variation. Again, the solutions are convergent, as Fig. 2 shows, and the predicted radial secular variation resembles that of paper 1, although there is considerably more small-scale structure in the Pacific hemisphere. The difference in values of $\oint_{CMB}\dot{B}_r^2\,d\Omega$ seems large, but is it significant? In fact, we chose to answer a slightly different question, namely: is the increase in residual norm necessary to produce a solution norm of 67.8 significant? The required residual norms are 2607 (DGRF) and 2592

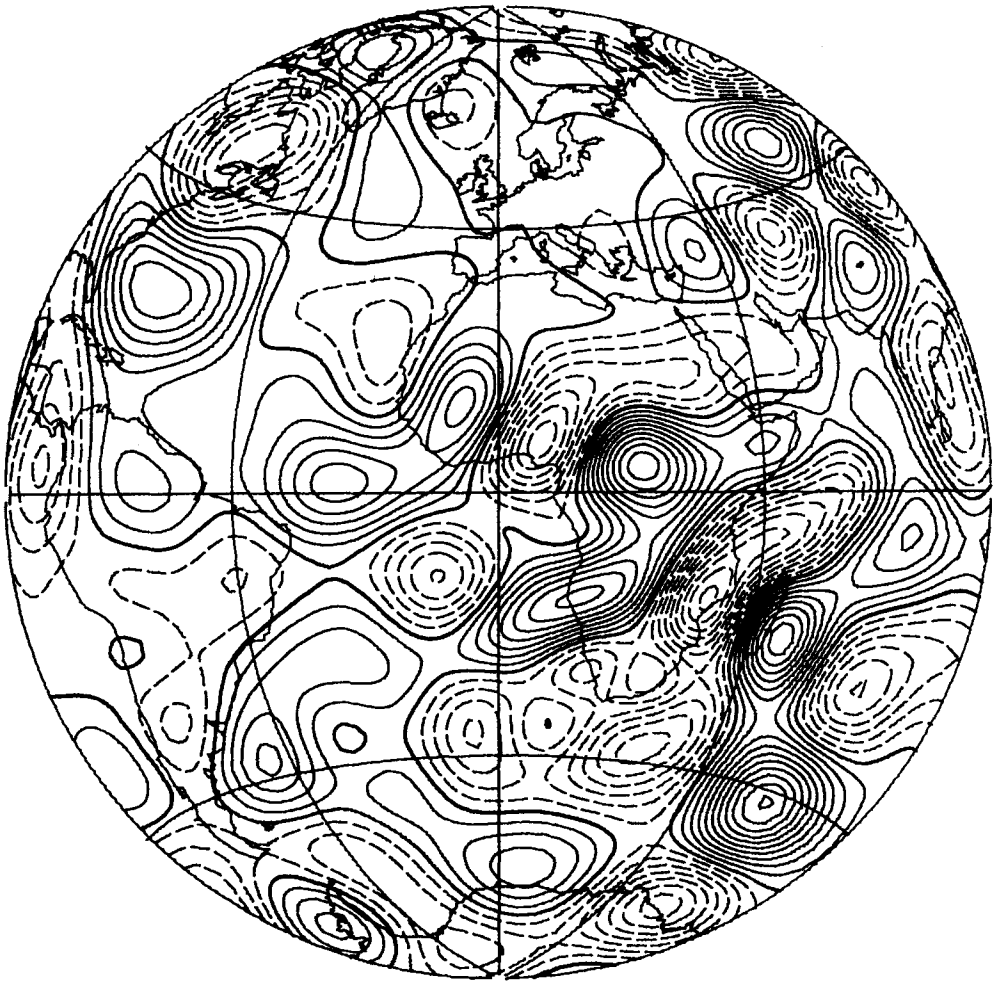

Figure 3. Radial CMB secular variation generated by model T1 on a Lambert equal area projection. The contour interval is 2000 nT yr $^{-1}$, i.e. double that of the maps of paper 1. Positive contours are continuous, negative contours dashed, thicker lines are zero contours.

(N1966(12)), again a factor of 2 larger than in the direct inversion. They should be distributed as χ^2 on the number of degrees of freedom of the solution, which is 318 (the number of data) minus the trace of the resolution matrix. An F-test indicates whether they are samples from the same distribution, or whether the purely toroidal velocity model value is significantly larger. The traces of the required resolution matrices are 66 (for solution T4) and 63 (solution T8). Ratios of 2.00 on 252, 318 and 2.90 on 255, 318 degrees of freedom are indeed significant, at the 100.00 per cent level (quoting the result to five significant figures), which implies that the null hypothesis of the residuals between the model and data are the same for the two pairs of models can be totally rejected. Note that this result does not depend on the estimates of the data residuals being correct, since any constant factors cancel. Thus the extra average 1 nT yr^{-1} residual pointed out by Shure *et al.* (1983) should not affect the conclusions.

Figure 3 – *continued*

This would appear to be very strong evidence against the 'no upwelling' hypothesis. The result is insensitive to the choice of main field model, implying that errors in the CMB radial field are unlikely to negate this conclusion. There are two other possibilities that can be investigated. Firstly, there may be no flow of the form (5) capable of fitting the data or, secondly, the numerical stabilizing of the solution explains the increase in $\oint_{\mathrm{CMB}} \dot{B}_r^2 \, d\Omega$ value. The latter possibility seems unlikely, since altering the very small number used to stabilize (norms (13) or (15) with damping factor λ in (18) varying between 10^{-6} and 10^{-10}) produced negligible change in $\oint_{\mathrm{CMB}} \dot{B}_r^2 \, d\Omega$. Both can be examined by including poloidal terms in the velocity expansion.

For a full velocity expansion, norms (13) and (15) again produce convergent solutions (for both the velocity and CMB radial secular variation) with values of $\oint_{\mathrm{CMB}} \dot{B}_r^2 \, d\Omega$ greater than that of paper 1. However, in this case they are only about 112 and 146 for the DGRF and 136 and 176 for N1966(12)) respectively (see Table 2). Also the power in the velocity field is considerably reduced (by at least an order of magnitude) when poloidal coefficients

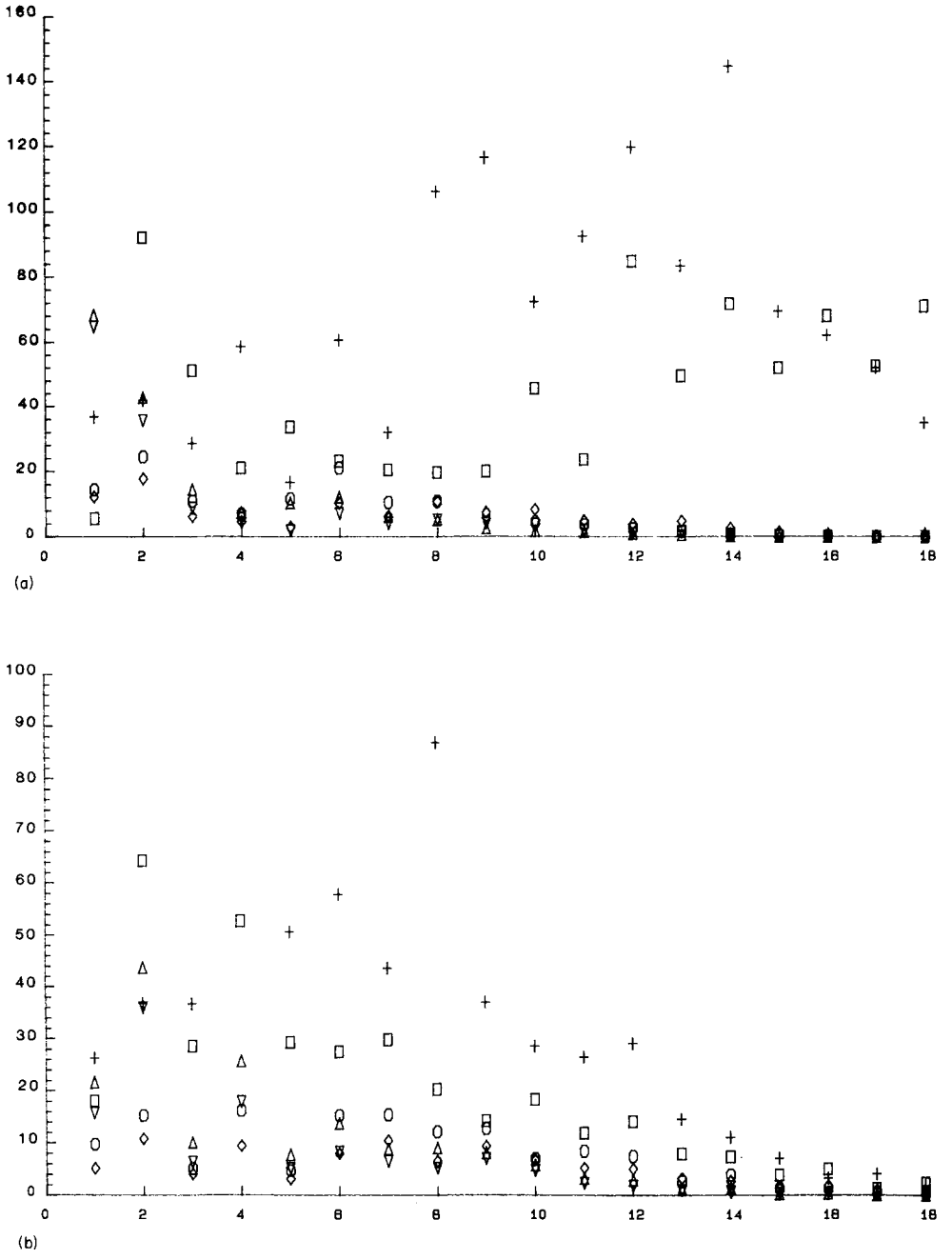

Figure 4. Power spectra for toroidal and poloidal flows. The velocity spectra for the toroidal and poloidal flows are shown separately. Likewise, the power spectrum of the radial CMB secular variation is split into the parts generated by the toroidal and poloidal parts of the flow. The toroidal and poloidal parts of both spectra are roughly equal, so there is no suggestion of weak upwelling and downwelling, or that the poloidal flow generates only a small part of the secular variation. (a) Toroidal velocity, (b) poloidal velocity, (c) radial CMB secular variation generated by the toroidal flow, (d) that generated by poloidal flow. TP1, △; TP2, ○; TP3, □; TP5, ▽; TP6, ◇; TP7, +. The harmonic degree 4 point is off the vertical scale for TP6 in part (b).

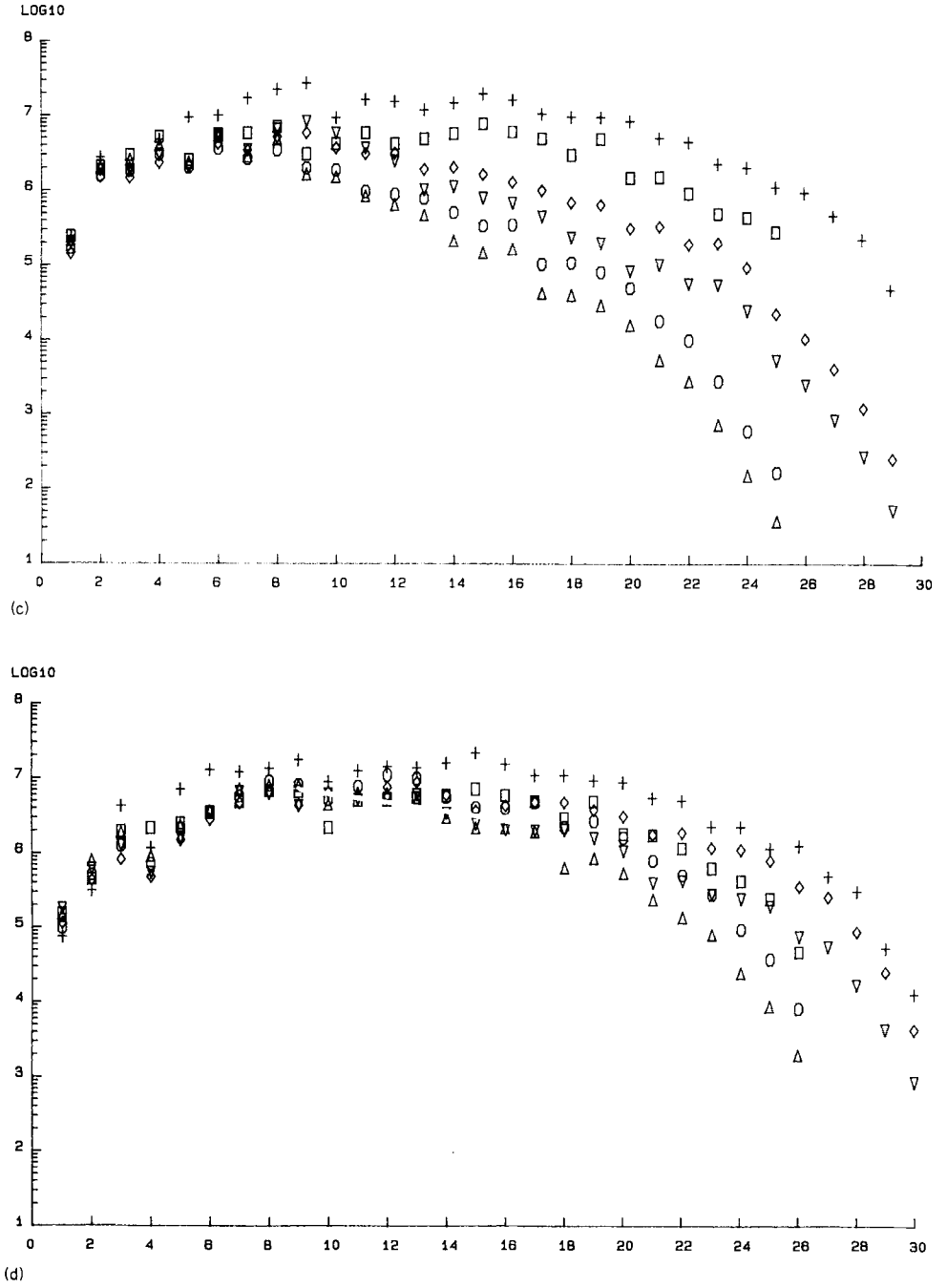

Figure 4 – *continued*

are included – see Fig. 4 which shows the toroidal and poloidal power separately. This shows that the power in the toroidal flow is roughly comparable with, rather than considerably larger than, that in the poloidal flow (a conclusion also reached by Gire *et al.* 1986). Likewise, the power in the secular variation generated by the toroidal and poloidal parts of

the flow separately is roughly comparable (see Fig. 4). Thus it is not the case that the observations of Whaler (1980, 1982) can be explained by weak upwelling and downwelling not resolved by the data and methods of those papers.

Again, we need to look at solutions minimizing $\oint_{CMB} \dot{B}_r^2 d\Omega$ to compare like with like. Once more, the system of equations is numerically unstable, and small numbers were added to the diagonal of the normal equations matrix. The (nearly) minimum values of $\oint_{CMB} \dot{B}_r^2 d\Omega$ are 71.0 (DGRF) and 81.6 (N1966(12)), only a few per cent larger than that of paper 1. Thus, the numerical stabilization is not responsible for the large value $\oint_{CMB} \dot{B}_r^2 d\Omega$ in the purely toroidal case. For the $\oint_{CMB} \dot{B}_r^2 d\Omega$ value of paper 1, the residual norms only need to be increased to 1332 and 1460, and the traces of the corresponding resolution matrices are 91 and 86. An F-test shows no statistically significant difference between the sums of squares of residuals in this case, demonstrating that there is at least one flow which adequately explains the data (thereby verifying the decomposition (5) of **v** at the CMB). Unless errors due to the non-zero conductivity of the mantle and/or flux not being frozen-in at the CMB have caused a false negative result of the F-test on the toroidal solutions, there is no alternative but to accept the implications of the F-tests on the purely toroidal solutions, i.e. there is upwelling at the CMB.

The power spectra for models TP3 and TP7 are also shown in Fig. 4. The toroidal part of the velocity is not convergent for model TP3, oscillating from about degree 14 onwards, although a solution obtained when the series was truncated instead at degree 14 appeared to be tending towards convergence. Thus, it is probably an instability arising with the DGRF, as model TP7 using N1966(12) shows normal convergent behaviour.

Since the secular variation is generated by advecting the main field by a specified velocity field in the frozen-flux approximation, it should be consistent with the constraints (3). These patch integrals were evaluated numerically as a check on the calculation of the equations of condition matrix, **B**, of equation (7), which relates velocity to secular variation coefficients.

Initially, a rather imprecise method was used, whereby a rectangular region of integration in (ϑ, ϕ) space was defined containing the patch, and the integrand at any point within was set to zero if B_r took the wrong sign, i.e. was outside the patch. This method has been used in previous evaluations of, and constraints on, the patch integrals (e.g. Shure *et al.* 1983; Gubbins 1983, 1984; Bloxham & Gubbins 1986). This was not adequate for present purposes – integrals of predicted secular variation over patches bounded by null-flux curves were not small, for instance, the magnitude of the two almost hemispheric patch integrals was about 500. Instead, a numerical zero-finding routine (applied to B_r) was used to find the ϕ limits of the patches at each ϑ value. Besides being more accurate, the method is more efficient numerically, since B_r does not have to be calculated at every point of a rectangular region to determine its sign – once the ϕ limits have been determined, for given ϑ, all points between them lie within the patch. In a further improvement, integrals over the almost hemispheric regions were calculated using analytic expressions for integrals of the spherical harmonics over hemispheric patches given by Gubbins (1983), and adding or subtracting the integrals over the regions contained between the undulations of the magnetic about the geographical equator, calculated as described above, and the patches nested within, as appropriate. This reduced absolute values of integrals of secular variation by an order of magnitude, to the values of about 50 presented in Table 3.

One final point which emerged during these calculations will be briefly mentioned here. Gire *et al.* (1984) have estimated the westward drift velocity of core fluid by a variety of techniques, some closely similar to that discussed here. They investigated varying the harmonic dependence of terms of a diagonal model covariance matrix using forms similar to

Table 3. Integrals of various secular variation models, or secular variation generated by velocity models, over patches of the CMB bounded by null-flux curves. The patches are named and numbered according to the region of the Earth's surface below which they lie (see, e.g. Bloxham & Gubbins 1986). The first three rows are taken from Shure *et al.* (1983), the fourth from paper 1, and used inaccurate calculations of the patch integrals of the spherical harmonics. However, recalculations performed using the more accurate method presented here do not change the order of magnitude of the values obtained for the previously published models.

Main field	Secular Variation	Patch Integrals ($nTyr^{-1}$)										
		Patch 2 S. of magnetic equator	1 N. of magnetic equator	South* Africa	South* America	N.W. Pacific	N. Pole	S. Pole	St. Helena	N.E. Pacific	Easter Island	N. Atlantic
DGRF	DGRF	609	-374	90	-143	-128						
IGRF	IGRF	497	-635	289	-169	47						
DGRF	Shure et al. (1983) $2nTyr^{-1}$ misfit	536	-602	62	-9	40						
DGRF	Paper 1	687	-489	-28	-39	-22						
DGRF	T4	34	-26	-4	0.7	0.7						
DGRF	TP1	56	-53	-3	1.3	0.3						
N1966(12)	T2	33	-63	29		-0.1	-4	-4	8	0.0	0.0	1.2
N1966(12)	TP3	101	-73	-29		0.1	-1	1	0.4	-0.4	0.0	0.2

* Numbers appearing midway between these two columns are for the N1966(12) main field, in which these two patches are amalgamated.

(13) and (15). They found that the value of t_1^0, the westward drift velocity, did not vary much whatever inversion method was used, and it was always the largest coefficient in the expansion. Having forced the velocity field to be primarily of low harmonic degree and order, through the choice of *a priori* covariance matrix, and finding that these results were broadly similar regardless of exactly how the diagonal covariance matrix was specified, they concluded that, if the motion was primarily of this form, as opposed to, say, turbulent motion, their value of t_1^0 was indeed representative of the drift of the CMB fluid, and this is the dominant motion. Table 4 gives the t_1^0 values of the full flow models presented here (purely toroidal motions are not considered since we have had to reject them); they are all smaller than Gire *et al.*'s (1984) for 1970. More interestingly, for models TP3 and TP4, t_1^0 is not the largest coefficient; for instance, $t_1^{1(s)}$, t_2^0, $t_2^{1(c)}$ and t_3^1, where the superscripts (s) and (c) denote the coefficient multiplying $\sin m\phi$ and $\cos m\phi$, are all larger in magnitude than t_1^0 for

Table 4. t_1^0, in $^\circ yr^{-1}$, for the full flows calculated here. The values are all negative indicating westward drift, but this is not the predominant motion in all the flows obtained. Subscripts (c) and (s) in the third column indicate the coefficient multiplying $\cos m\phi$ and $\sin m\phi$ respectively.

Model	t_1^0 ($^\circ yr^{-1}$)	Coefficients greater than t_1^0 in magnitude
TP1	−0.047	–
TP2	−0.022	–
TP3	−0.011	t_2^0, t_2^1, $t_2^{2(c)}$, t_3^0, t_3^1
TP4	−0.012	$t_1^{1(s)}$, t_2^0, $t_2^{1(c)}$, t_3^1
TP5	−0.046	–
TP6	−0.020	–
TP7	−0.035	–
TP8	−0.033	–

model TP4. This casts doubt on the conclusions of Gire *et al.* (1984) since (18) is a valid norm of **v**, broadly satisfying their requirements of large-scale, ordered flow, yet it produces very little westward drift.

5 Discussion

The main conclusion of this paper is that there is fluid upwelling and downwelling at the CMB. This is resolvable by the method described here even with the relatively small dataset investigated, whereas other methods applied to the same data have been unable to distinguish between hypotheses. The result is not affected by the non-uniqueness of the CMB velocity determined geomagnetically.

The method involves solving a parameter by parameter system of linear equations, so is capable of handling large datasets. Since most secular variation data are obtained from magnetic observatory records, the maximum number is unlikely to be more than, say, a factor of 2 larger. The 15 yr timespan, 1959–74, used to obtain the secular variation data used here is larger than ideal, especially as it spans the geomagnetic 'jerk' of about 1970, which may be associated with a change in magnetic field and/or velocity geometry. Also, it is impossible to fit these secular variation data to within their estimated errors calculated by Shure *et al.* (1983), so they may be contaminated by external fields. Thus it is desirable to apply the method to a different dataset to confirm the results.

A second area in which the results of the present study might eventually be improved on is to relax the assumptions of an insulating mantle and perfectly conducting core. The electrical conductivity of the mantle is too poorly known, and earlier field models, with relatively low truncation levels, too inaccurate at the CMB, to make these calculations worthwhile at the moment. This situation may change with the availability of what are believed to be more accurate recent models (e.g. Bloxham & Gubbins 1986). The effects of finite core conductivity can easily be taken into account in the method described here. Retaining the Ohmic diffusion term in the induction equation contributes an easily evaluated constant term on the right side. This term depends on the (unknown) jump in $\partial B_r/\partial_r$ across the CMB but, if this is specified, the extra term can be incorporated into the data on the left side to give new 'effective' data.

No physical significance can be attached to the flows presented here because of the non-uniqueness of the velocity determined using the frozen-flux form of the radial component of the induction equation. Thus we cannot address the question as to where the upwelling and downwelling occurs. Likewise, the values of the torodial coefficient t_1^0 from this method do not represent westward drift of the fluid layers adjacent to the CMB. Predominantly low degree motion produces a wide variety of t_1^0 values, and this need not be the dominant term in the expansion, depending on how *a priori* information is specified.

The method developed here can be adapted to find the steady (i.e. constant with time) part of the motion, whose uniqueness has recently been proved (Voorhies 1984). Main field models and secular variation data from several epochs can be fed into equation (7) with the same velocity coefficients, independent of epoch, as the model parameters. Each secular variation datum defines an equation of condition, and the inversion of the larger dataset will then determine the steady part of the motion. Different norms, e.g. minimizing the power in the time-varying part of the flow, may be more appropriate than those used here.

Acknowledgments

This work was begun while the author held a NERC personal fellowship at the Bullard Laboratories, University of Cambridge. Thanks to Denis Winch for providing the FORTRAN

function used to calculate the Wigner 3-*j* coefficients, and comments on its use in evaluating the Elsasser and Gaunt integrals, to David Gubbins for providing the coefficients of his unpublished 1966 main field model; and to J.-L. Le Mouël for a copy of his recent work prior to publication. Discussions with Jeremy Bloxham, David Crossley and David Gubbins are also gratefully acknowledged.

References

Backus, G. E., 1968. Kinematics of geomagnetic secular variation in a perfectly conducting core, *Phil. Trans. R. Soc. A*, **263**, 239–266.

Backus, G. E. & Gilbert, F., 1968. The resolving power of gross Earth data, *Geophys. J. R. astr. Soc.*, **16**, 169–205.

Barraclough, D. R., Harwood, J. M., Leaton, B. R. & Malin, S. R. C., 1978. A definitive model of the geomagnetic field and its secular variation for 1965 – I. Derivation of model and comparison with IGRF, *Geophys. J. R. astr. Soc.*, **55**, 111–121.

Benton, E. R., 1981. A simple method for determining the vertical growth rate of vertical motion at the top of Earth's outer core, *Phys. Earth planet. Int.*, **24**, 242–244.

Benton, E. R. & Whaler, K. A., 1983. Rapid diffusion of the poloidal geomagnetic field through the weakly conducting mantle: a perturbation solution, *Geophys. J. R. astr. Soc.*, **75**, 77–100.

Bloxham, J. & Gubbins, D., 1986. Geomagnetic field analysis – IV. Testing the frozen-flux hypothesis, *Geophys. J. R. astr. Soc.*, **84**, 139–152.

Bullard, E. C. & Gellman, H., 1954. Homogeneous dynamos and terrestrial magnetism, *Phil. Trans. R. Soc. A*, **247**, 213–278.

Gibson, R. D. & Roberts, P. H., 1969. The Bullard–Gellman dynamo, in *Applications of Modern Physics to the Earth and Planetary Interior*, pp. 577–602, ed. Runcorn, S. K.

Gire, C., Le Mouël, J.-L. & Madden, T., 1984. The recent westward drift rate of the geomagnetic field and the body drift of external layers of the core, *Annls Geophys.*, **2**, 37–45.

Gire, C., Le Mouël, J.-L. & Madden, T., 1986. Motions at the core surface derived from *SV* data, *Geophys. J. R. astr. Soc.*, **84**, 1–29.

Gubbins, D., 1982. Finding core motions from magnetic observations, *Phil. Trans. R. Soc. A*, **306**, 247–254.

Gubbins, D., 1983. Geomagnetic field analysis – I. Stochastic inversion, *Geophys. J. R. astr. Soc.*, **73**, 641–652.

Gubbins, D., 1984. Geomagnetic field analysis – II. Secular variation consistent with a perfectly conducting core, *Geophys. J. R. astr. Soc.*, **77**, 753–766.

Gubbins, D. & Bloxham, J., 1985. Geomagnetic field analysis – III. Magnetic fields on the core–mantle boundary, *Geophys. J. R. astr. Soc.*, **80**, 695–713.

Gubbins, D., Thomson, C. J. & Whaler, K. A., 1982. Stable regions in the Earth's liquid core, *Geophys. J. R. astr. Soc.*, **68**, 241–251.

Kahle, A. B., Vestine, E. H. & Ball, R. H., 1967. Estimated surface motions at the core surface, *J. geophys. Res.*, **72**, 1095–1108.

Madden, T. & Le Mouël, J.-L., 1982. The recent secular variation and motions at the core surface, *Phil. Trans. R. Soc. A*, **306**, 271–280.

Roberts, P. H. & Scott, S., 1965. On analysis of the secular variation, 1 A hydromagnetic constraint: theory, *J. Geomagn. Geoelect.*, **17**, 137–151.

Shure, L., Whaler, K. A., Gubbins, D. & Hobbs, B. A., 1983. Physical constraints for the analysis of the secular variation, *Phys. Earth planet. Int.*, **32**, 114–131.

Voorhies, C. V., 1984. Magnetic location of Earth's core–mantle boundary and estimates of the adjacent fluid motion, *PhD thesis*, University of Colorado at Boulder.

Voorhies, C. V. & Backus, G. E., 1985. Steady flows at the top of the core from geomagnetic field models: the steady motions theorem, *Geophys. Astrophys. Fluid Dyn.*, **32**, 163–173.

Whaler, K. A., 1980. Does the whole of the Earth's core convect? *Nature*, **287**, 528–530.

Whaler, K. A., 1982. Geomagnetic secular variation and fluid motions at the core surface, *Phil. Trans. R. Soc. A*, **306**, 235–246.

Whaler, K. A., 1984. Fluid upwelling at the core–mantle boundary – resolvability from surface geomagnetic data, *Geophys. J. R. astr. Soc.*, **78**, 453–473.

Whaler, K. A. & Gubbins, D., 1981. Spherical harmonic analysis of the geomagnetic field: an example of a linear inverse problem, *Geophys. J. R. astr. Soc.*, **65**, 645–693.

Wigner, E. P., 1959. *Group Theory and its Applications to the Quantum Mechanics of Atomic Spectra*, Academic Press, New York.

Winch, D. E., 1974. Evaluation of geomagnetic dynamo integrals, *J. Geomagn. Geoelect.*, **26**, 87–94.

Zmuda, A. J., 1971. World magnetic survey 1957–1969, *IAGA Bull. No. 28.*